

See discussions, stats, and author profiles for this publication at: <https://www.researchgate.net/publication/10869641>

Flow Injection Analysis in a Microfluidic Format

ARTICLE *in* ANALYTICAL CHEMISTRY · MARCH 2003

Impact Factor: 5.64 · DOI: 10.1021/ac026112l · Source: PubMed

CITATIONS

70

READS

41

3 AUTHORS:



[Andrew Leach](#)

GE Global Research

36 PUBLICATIONS 1,003 CITATIONS

[SEE PROFILE](#)



[Aaron R Wheeler](#)

University of Toronto

130 PUBLICATIONS 4,616 CITATIONS

[SEE PROFILE](#)



[Richard Zare](#)

Stanford University

1,151 PUBLICATIONS 43,928 CITATIONS

[SEE PROFILE](#)

Flow Injection Analysis in a Microfluidic Format

Andrew M. Leach, Aaron R. Wheeler, and Richard N. Zare*

Department of Chemistry, Stanford University, Stanford, California 94305-5080

A microfluidic flow injection analysis system has been designed and evaluated. The system incorporates within a single two-layer poly(dimethylsiloxane) monolith multiple pneumatically driven peristaltic pumps, an injection loop, a mixing column, and a transparent window for fluorescence detection. Central to this device is an injection system that mimics the operation of a standard six-port, two-way valve used in conventional liquid chromatography and flow injection experiments. Analyte and carrier solutions continuously flow through this injection system allowing for measurements and sample changes to be performed rapidly and simultaneously. Injection volumes of 1.25 nL generated peak area reproducibility of better than 3% relative standard deviation. The flow injection device was evaluated with fluorescent dyes and demonstrated a detection limit of 400 zmol for fluorescein. A rudimentary sample selection system allowed calibration curves to be rapidly produced, often in less than 10 min. The hydrolysis of fluorescein diphosphate by alkaline phosphatase demonstrates that chemical assays can be carried out with this device in a manner characterized by short analysis times and low sample consumption.

The recent trend toward miniaturized chemical assays has led to the development of the field of micro total analysis systems (μ TAS).^{1,2} Integration of the procedures performed by an entire laboratory onto a single microfluidic chip promises the ability to produce high-throughput, parallel systems ideally suited for automation. The small scale of μ TAS experiments results in a dramatic reduction in solution consumption, meaning that lower sample volumes are required and less waste is generated. Improved fabrication techniques and the use of new materials has helped the field move toward its ultimate goal of producing low-cost, disposable instrumentation.

Flow injection analysis (FIA) is a widely used sampling system that has great potential for miniaturization.^{3,4} In FIA experiments, a known sample volume is injected into a flowing stream of solution, commonly called the carrier. Flow injection systems often

incorporate a range of operations including dilution or mixing, analyte enrichment, chemical labeling, matrix modification, and solvent exchange.^{3,4} Experiments are typically automated for the generation of rapid, highly reproducible results. Flow injection systems consist of pumps, an injection valve, a mixing column, and a detector.

Several research efforts have been directed toward the development of miniaturized FIA devices. Most experiments have incorporated microfluidic channels and mixing schemes coupled with macroscale injection valves and pumps.^{5,6} Although this approach has produced intriguing results, several key properties of μ TAS, including integration and low sample consumption, are lost. Ramsey and co-workers⁷ demonstrated the use of electrokinetic pumping and injection for an entirely microscale enzymatic assay. This study showed that solutions that contained large molecules with low diffusion constants could achieve sufficient mixing in moderate length channels. Additionally, electrokinetic injection allowed several concentrations of one analyte to be introduced to the mixing system to generate a rapid calibration technique. The use of electrokinetic pumping, however, placed restrictions on the electrolyte composition of solutions. Veenstra et al.⁸ have recently demonstrated the incorporation of miniaturized peristaltic pumps and fluidic channels within a monolithic device for the determination of ammonium concentration.

The recent development of microvalves^{9–12} allows for the reliable control and distribution of solutions within microfluidic networks. Traditionally, most miniaturized valves have been based on the combination of a flexible diaphragm with an electromechanical actuator.⁹ Diaphragm valves provide a robust means of flow control but have limited movement range and require complicated fabrication techniques. Hydrogel-based microvalves

* To whom correspondence should be addressed: (e-mail) zare@stanford.edu.

- (1) Reyes, D. R.; Iossifidis, D.; Auroux, P.-A.; Manz, A. *Anal. Chem.* **2002**, *74*, 2623–2636.
- (2) Auroux, P.-A.; Iossifidis, D.; Reyes, D. R.; Manz, A. *Anal. Chem.* **2002**, *74*, 2637–2652.
- (3) Ruzicka, J.; Hansen, E. H. *Flow Injection Analysis*; John Wiley & Sons: New York, 1981.
- (4) Trojanowicz, M. *Flow Injection Analysis Instrumentation and Applications*; World Scientific: Singapore, 2000.

- (5) Emnéus, J.; Yakovleva, J.; Davidsson, R.; Lobanova, A.; Eremin, S.; Laurell, T.; Bengtsson, M. In *Proceedings of Micro Total Analysis Systems 2001*; Kluwer Academic Publishers: Dordrecht, The Netherlands, 2001; pp 432–434.
- (6) Kerby, M.; Chien, R. L. In *Proceedings of Micro Total Analysis Systems 2001*; Kluwer Academic Publishers: Dordrecht, The Netherlands, 2001; pp 625–626.
- (7) Hadd, A. G.; Raymond, D. E.; Halliwell, J. W.; Jacobson, S. C.; Ramsey, J. M. *Anal. Chem.* **1997**, *69*, 3407–3412.
- (8) Veenstra, T. T.; Tiggelaar, R. M.; Sanders, R. G. P.; Berenschot, J. W.; Gardeniers, J. G. E.; Wissink, J. M.; Mateman, R.; Elwenspoek, M. C.; van den Berg, A. In *Proceedings of Micro Total Analysis Systems 2001*; Kluwer Academic Publishers: Dordrecht, The Netherlands, 2001; pp 664–666.
- (9) Kovacs, G. T. A. *Micromachined Transducers Sourcebook*; WCB McGraw-Hill: New York, 1998.
- (10) Jo, B.-H.; Moorthy, J.; Beebe, D. J. In *Proceedings of Micro Total Analysis Systems 2000*; Kluwer Academic Publishers: Dordrecht, The Netherlands, 2000; pp 335–338.
- (11) Liu, R. H.; Yu, Q.; Beebe, D. J. *J. Microelectromech. Syst.* **2002**, *11*, 45–53.
- (12) Unger, M. A.; Chou, H.-P.; Thorsen, T.; Scherer, A.; Quake, S. R. *Science* **2000**, *288*, 113–116.

that swell in response to a variety of external stimuli offer an exciting means of regulating liquid movement but have response rates too slow for rapid analyses.^{10,11} Quake and co-workers¹² have reported pneumatic valves constructed in multilayer poly(dimethylsiloxane) (PDMS) devices. These PDMS valves consist of overlapped fluidic and control channels (that reside in different layers) that are separated by a thin polymeric membrane. Increased pressure in the control channel results in the deformation of the PDMS membrane and closing of the fluidic channel. Simple valves and peristaltic pumps produced by a series of valves have been demonstrated using this technology.

In this study, a monolithic FIA system has been demonstrated that incorporates peristaltic pumps, an injection valve, and a mixing column. A critical component of this device is a microfluidic injection loop that operates in a manner similar to a standard six-port, two-way injection valve commonly used in liquid chromatography and flow injection experiments. This flow-through injection system provides a simple, robust method for the introduction of a geometrically defined sample volume (1.5 nL in this experiment) to the carrier stream. An additional set of microvalve controls allow a combination of two samples that are different in chemical composition or concentration to be delivered to the injection region. The enzymatic hydrolysis of fluorescein diphosphate by alkaline phosphatase demonstrates the ability of this microfluidic FIA device to perform rapid, sensitive assays with limited sample consumption.

EXPERIMENTAL SECTION

Reagents and Solutions. All solutions were prepared in 18-M Ω deionized water (Millipore, Bedford, MA). A 1% solution of the nonionic surfactant Triton X-100 (Sigma Chemical Co., St. Louis, MO) was used to initially wet the PDMS fluidic channels. Borate buffer was prepared with boric acid (Mallinckrodt, Inc., Paris, KY) and brought to a pH of 9.1 with sodium hydroxide (Mallinckrodt Baker, Inc., Paris, KY). Fluorescein (Aldrich Chemical Co., Inc., Milwaukee, WI) and fluorescein diphosphate (Molecular Probes, Inc., Eugene, OR) standards were made by serial dilution in 10 mM borate buffer. A 10% solution of bovine albumin labeled with fluorescein isothiocyanate (Sigma Chemical Co.) used in mixing studies was prepared in water. Alkaline phosphatase (bovine intestinal mucosa, Sigma Chemical Co.) solutions were made in borate buffer and refrigerated when not in use. A 1% solution of bovine albumin (Sigma Chemical Co.) that was used to reduce enzyme adhesion to the PDMS channels was prepared in deionized water. The mixing column was filled with the albumin solution for 1 h and then rinsed with deionized water prior to enzyme measurements.

Device Fabrication. The microfluidic FIA manifold (Figure 1) used throughout this study was designed with FluidArchitect Design Software (version 1.0, Fluidigm Corp., South San Francisco, CA) and fabricated by Fluidigm with soft lithography techniques.¹³ Operation of polymeric microvalves and peristaltic pumps similar to those used in this study has been previously reported by Quake and co-workers.¹² The FIA devices consisted of two PDMS layers that are permanently bonded together. Fluidic channels that are 100 μm wide and 10 μm in height (measured in the center of the channel) are formed within a thin film ($\sim 30 \mu\text{m}$)

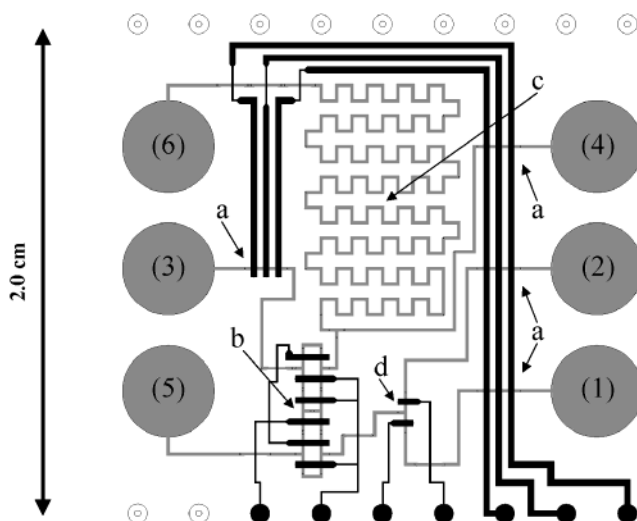


Figure 1. Diagram of the multilayer PDMS microfluidic flow injection analysis system. Fluidic channels are shown in gray, and control channels (pumps and valves) in black. Fluidic components include (a) peristaltic pumps, (b) injection valve, (c) mixing/reaction column, and (d) sample selector. The six fluid reservoirs contained (1, 2) two sample solutions, (3) carrier, (4) reactant, (5) sample waste, and (6) mixing column waste.

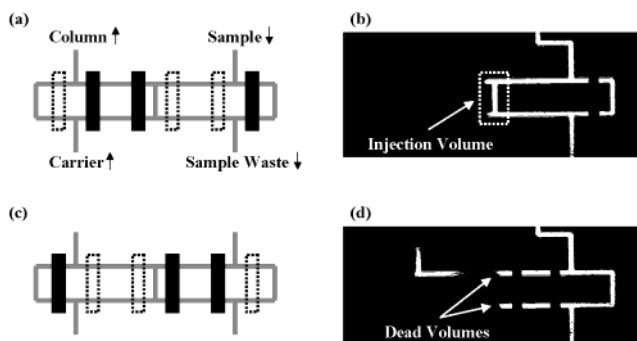


Figure 2. Operation of the microfluidic injection loop in the load (a) and inject (c) positions. Fluidic channels are shown in gray, and microvalves are in black. A solid black bar signifies a closed valve; a dotted outline is an open valve. The valve system was imaged in the load (b) and inject (d) positions with 1 mM fluorescein dye. The dotted white rectangle in (b) represents the injection volume.

of PDMS. Control lines (200 μm wide) are molded in a thick layer ($\sim 5000 \mu\text{m}$) of PDMS and positioned above the fluidic channels. A thin membrane of polymer separated the fluidic and control channels and allowed for the actuation of pumps and valves. The PDMS chips were bonded to a glass cover slip that acted as the final wall for the microfluidic channels and provided a window for optical imaging. The entire device measures 2.0 cm by 2.0 cm.

A key component of this FIA chip is the low-volume injection loop, seen in Figure 2. This injection system is operated in a manner similar to a standard six-port, two-way valve commonly used in liquid chromatography and flow injection experiments. The injection loop consists of two inputs and two outputs connected by multiple fluidic channels. Two sets of valves are used to control the state of the injection system, with one set of valves closed at all times. In the load position (Figure 2a,b) one set of valves is closed, forcing the sample to flow through the injection volume while the carrier bypasses the loop and enters the mixing

(13) Quake, S. R.; Scherer, A. *Science* **2000**, *290*, 1536–1540.

column. To inject a sample, the state of the valves is reversed (Figure 2c,d), directing the carrier through the analyte-filled injection volume and into the mixing column. Because both the sample and carrier are constantly pumped, the injection loop is refilled while the previous injection continues to move through the mixing region. The injected volume of this system is calculated to be 1.5 nL (see Figure 2b).

Instrumentation. The PDMS devices were placed on an inverted microscope (Axiovert 135, Zeiss) equipped with a motorized x - y positioning stage (Prior, model H107, Rockland, MD). Excitation at 488 nm was provided by an argon ion laser (Melles Griot, model 35 LAP-431-208, Carlsbad, CA). A laser power of 700 μ W (measured at the microfluidic device) was used in all experiments. The excitation light was reflected by a dichroic mirror and focused on the chip with a 40 \times objective (LD Achromplan, model 44 08 64, Zeiss). Fluorescence was collected by the same objective and transmitted through the dichroic mirror and a band-pass filter (HQ 535/50M, Omega Optical, Inc., Brattleboro, VT). Spatial filtering of the excitation region was provided by a 0.05-in.-diameter pinhole positioned in front of the photomultiplier detector (R4632, Hamamatsu, Bridgewater, NJ). Signal was measured with a picoammeter (model 845, Keithley Instruments, Cleveland, OH) and recorded with LabVIEW software operated on a PC computer. Images were collected with a CCD camera (LCL-802H, Watec, Las Vegas, NV), recorded with a VCR, and manipulated with ScionImage software (Version 4.0.2, Scion Corp., Frederick, MD).

Pneumatic pressure to the PDMS devices was controlled with a FluidController valve controller (Fluidigm). Helium (99.99%, Praxair, Danbury, CT) at a pressure of 20 psi was used to actuate the microvalves. As discussed in detail in the next section, deionized water was used in lieu of helium in some valve control lines to limit gas bubble formation in the FIA fluidic channels.

RESULTS AND DISCUSSION

Flow Rate. The microfluidic peristaltic pumps are composed of three discrete valves that open and close in a specific sequence to force fluid in a chosen direction.^{12,14} The time required for an injected plug of fluorescein dye to travel a known distance was used to calculate the flow rate produced by the carrier solution peristaltic pump as a function of pump frequency (see Figure 3). Volumetric flow rate increased with elevated pump frequency to 6 Hz, where a maximum flow rate of 21 nL min⁻¹ was achieved. Higher pump frequencies resulted in a dramatic reduction in flow rate. Visual inspection confirmed that as the pump frequency is increased beyond 6 Hz at least one of the three valves failed to open completely, resulting in a loss of fluid movement.

Quake and co-workers¹² reported similar losses in pump efficiency at frequencies greater than 70 Hz. Although the trend seen in Figure 3 corresponds well with this previously reported behavior, the absolute frequency at which pump efficiency plateaus and declines is very different. The explanation for this deviation is the different flow resistance of the pump control lines. Flow resistance increases linearly with channel length and to the fourth root with channel radius.¹⁵ In the current experiment, relatively

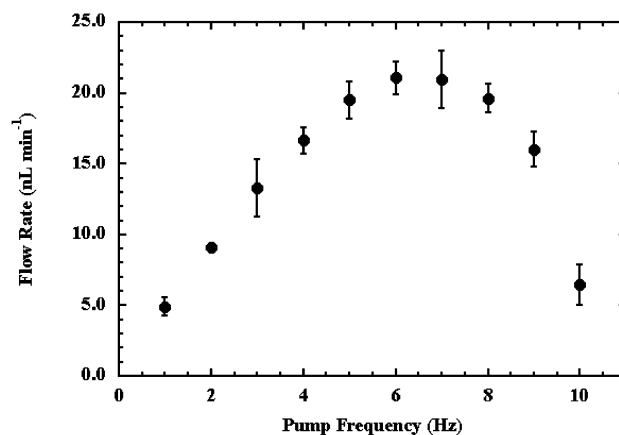


Figure 3. Flow rate generated by pneumatically driven peristaltic pumps as a function of operating frequency. Error bars denote three times the standard deviation of the flow rate measurement.

long control channels were required to operate simultaneously four separate peristaltic pumps. Although control channel width was maximized (200 μ m) in most situations to limit flow resistance, the width was reduced to 50 μ m at one location (near reservoir 6 in Figure 1) to bridge a fluidic channel without formation of a valve. This short length of narrow channel accounted for \sim 45% of the flow resistance in the pump lines.

As in previous microfluidic valve studies,^{12,14} nitrogen gas was initially used to actuate the control elements (valves and pumps). However, it was found that gas bubbles often formed in fluidic channels adjacent to control elements. A possible explanation for this phenomenon is the transport of the gas through the thin PDMS membrane that separates the fluidic and control channels. To overcome the bubble problem, the valves and pumps were evaluated with the control lines filled with water. Although no bubbles formed, the elevated viscosity of water significantly degraded the performance of the peristaltic pumps. Control lines filled with helium were also used to test the valves and pumps. With helium, bubbles were noticed when pressure was continuously applied, as in the case of valves, but not when the pressure was rapidly modulated, as with the peristaltic pumps. Thus, in the present study, helium was used in the pump control lines, and the valve control lines were filled with water.

The difference in behavior of helium (bubble formation near valves but not pumps) and nitrogen (bubbles formed near valves and pumps) can be explained by the different diffusion and solubility coefficients of the two gases in PDMS.¹⁶ Helium has a greater diffusion coefficient (largely owing to its smaller size) than nitrogen, but a lower solubility. When pressure is continuously applied, it is expected that helium will more rapidly diffuse through the membrane into the fluidic channels. However, the lower solubility of helium in PDMS indicates that as the pressure in the control line is reduced, the helium will more quickly return to the control line instead of continually migrating toward the fluidic channel.

Injection Loop Characterization. The injection system for this device was designed to mimic the performance of a standard six-port, two-way valve used in liquid chromatography and flow injection experiments. The macroscale valves are based on the

(14) Fu, A. Y.; Chou, H.-P.; Spence, C.; Arnold, F. H.; Quake, S. R. *Anal. Chem.* **2002**, *74*, 2451–2457.

(15) Potter, M. C.; Wiggert, D. C. *Mechanics of Fluids*, 3rd ed.; Brooks/Cole: Pacific Grove, CA, 2002.

(16) Barrer, R. M.; Chio, H. T. *J. Polym. Sci.* **1965**, *C10*, 111–138.

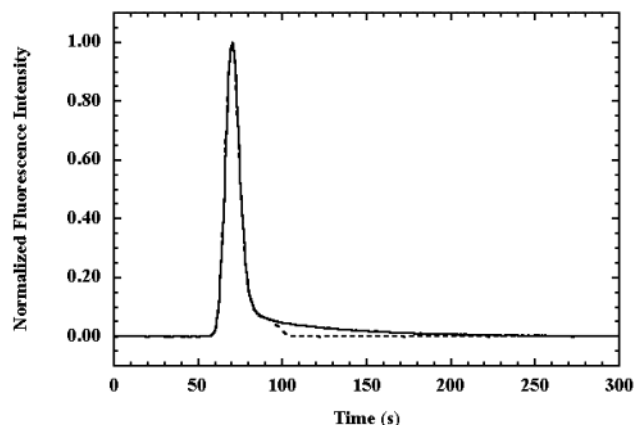


Figure 4. Temporal profile of 366 nM fluorescein plugs measured at 78.25 mm from the mixing point. The solid curve represents the sample pulse produced when the injection valve is left in the "inject" position for 600 s, while the dashed curve shows the truncated plug generated when the valve is returned to the "load" position after 30 s. A pump rate of 5.0 Hz was used.

ability to alter physically the position of a plate that contains six fluid input and output ports relative to a second plate in which three channels form connections between two adjacent ports. The amount of sample injected by these valves is highly reproducible because the length of tubing used to connect two of the ports defines geometrically the volume. Additionally, because the carrier and sample solutions are physically isolated from one another, the analyte composition can be changed without interrupting the carrier flow directed to the mixing column.

Figure 2 demonstrates the operation of the microfluidic injection loop. Because the position of the carrier and sample solution flows relative to the injection volume could not be physically changed within this system, a series of valves and alternate channels was used to produce liquid flow through the injection volume. The channel volume located between the two central valves defines the size of the injection loop (see Figure 2c). This volume is the combination of the length of the injection loop (seen as a vertical line in Figure 2) and the lengths of four input and output channels that are located within the region defined by the two microvalves. The injection loop used in this study has a calculated volume of 1.5 nL based on geometry.

As evident in Figure 2d, significant dead volumes are produced by the short lengths of channel from the sample source that become part of the injection loop in the inject mode. Reduction of the size of these stagnant regions is limited by fabrication requirements. Manual alignment of the fluidic and control layers during the manufacturing process mandates that an offset (200 μm at the time these devices were fabricated, but currently 50 μm) exist between fluid channels and valves. The calculated Reynolds number (Re) for this system typically ranges from 0.01 to 0.02, meaning that flow is highly laminar in profile. Under these conditions, diffusion will be responsible for mixing of the carrier solution with these analyte-filled dead volumes. The solid curve in Figure 4 shows the temporal profile of an injection of fluorescein dye into the carrier stream when the sample loop is left in the inject position indefinitely. Significant peak tailing that lasts more than 150 s is the result of diffusional mixing of the injector's dead volumes into the carrier stream. When the loop is returned to the load position 30 s after an injection (dashed curve in Figure

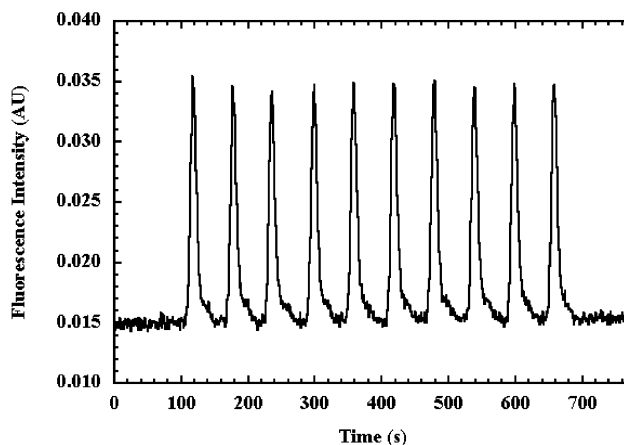


Figure 5. Reproducible injection of 10.6 nM fluorescein measured 78.25 mm from the mixing point. With an injection volume of 1.25 nL, each injection corresponds to 13.3 amol of dye. A pump rate of 5.0 Hz was used.

4), the tailing is truncated to produce a transient ~ 45 s in duration. The amount of analyte lost in these shortened injections is a function of the molecule's diffusion constant. Fluorescein has a relatively high diffusion constant ($4.25 \times 10^{-6} \text{ cm}^2 \text{ s}^{-1}$)¹⁷ and therefore can approximate the minimum lost analyte volume because the majority of the dye diffuses into the carrier stream before the injection loop position is changed. The shortened peak has an area 17% less than the untruncated peak, corresponding to an actual injected volume of 1.25 nL. Future improvements in chip manufacturing should result in a dramatic reduction in the injector's dead volume.

Figure 5 shows the repetitive injection of 10.6 nM fluorescein. Based on an injection volume of 1.25 nL each transient represents 13.3 amol of dye. Peak height and area relative standard deviations were calculated to be 1.9 and 2.2%, respectively. As seen in Figure 5, greater than 60 samples/h can be analyzed with this microfluidic FIA device. The limit of detection, defined as the concentration that produces a signal three times the standard deviation of the background, was calculated to be 400 zmol for fluorescein.

Sample Selector. In macroscale FIA experiments, samples are rapidly changed by placement of the pump tubing in a new solution. However, no microfluidic analogue exists for this procedure. A typical sample change requires that the fluid reservoir be emptied, rinsed, and refilled and the new solution be pumped to the appropriate location before a measurement. This time-consuming procedure increases analysis time and reduces sample throughput. Ideally, multiple samples would be simultaneously loaded into the microfluidic device, and then valves would be used to select which samples are injected and analyzed.

Figure 1 shows that the microfluidic FIA device incorporates a rudimentary sample selection system. Two samples are simultaneously loaded into adjacent fluid reservoirs. Peristaltic pumps force liquid toward a fluidic tee with two valves. The state of these valves determines the composition of the solution passed to the injection loop. With one valve open, the entire injection loop is filled with a single sample. With both valves open, the injected solution contains equal portions of both analytes. Figure 6 shows

(17) Culbertson, C. T.; Jacobson, S. C.; Ramsey, J. M. *Talanta* **2002**, *56*, 365–373.

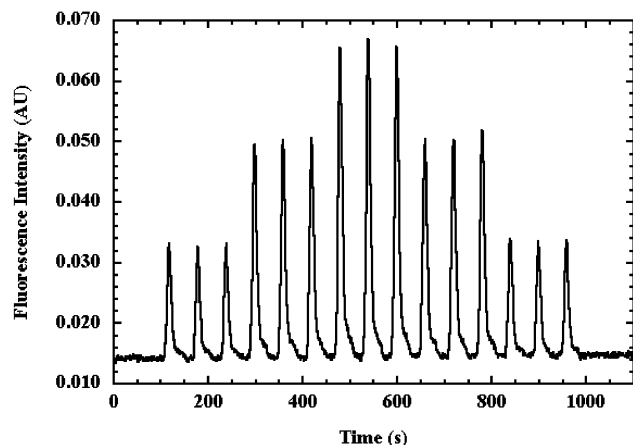


Figure 6. Replicate injections of fluorescein demonstrating the operation of the sample selector. Sample reservoirs 1 and 2 (see Figure 1) contained 10.6 and 41.0 nM fluorescein, respectively. Fluorescence was measured at 78.25 mm from the mixing point with a pump rate of 5.0 Hz.

the combination of intensities produced when two concentrations of fluorescein dye are loaded into reservoirs 1 and 2 (see Figure 1), and a sample selector valve sequence of 01, 11, 10, 11, 01 (0 = closed, 1 = open) is used. The extreme intensity peaks are 10.6 and 41.0 nM, while the intermediate peaks are the average of the low- and high-concentration solutions (25.8 nM). The best-fit regression of these data points exhibited good linearity with a coefficient (R^2) equal to 0.998. Additionally, the symmetry of Figure 6 shows that the memory effects associated with sample changes were minimal. Although the FIA device described here only incorporated two analyte solutions (concentrations), it is easy to envision a more elaborate system with many fluid reservoirs thus dramatically improving sample throughput.

Mixing/Reaction Column Characterization. The low Re typically encountered in microfluidic systems, often less than 1, yields highly laminar flow. Under these conditions, diffusion dominates radial mixing of the two coaxial liquid streams. With diffusion coefficients of $10^{-7} \text{ cm}^2 \text{ s}^{-1}$ for large molecules including proteins and DNA fragments, mixing times for small-dimension channels (100 μm wide) can be greater than 100 s.¹⁸ For these reasons, considerable effort has been directed toward the development of both active^{9,18} and passive^{9,19–21} microfluidic mixers.

The mixing channel seen in Figure 1 was designed with numerous right-angle turns in an effort to generate radial mixing. At higher Re (>100), serpentine channels have demonstrated considerable success in mixing laminar flows.¹⁹ At Re less than 1 (such as in this study), however, the geometry of the fluid channel has little effect on the mixing behavior.

Visual inspection confirmed that diffusion was the dominant form of mixing. Fluorescent dye was pumped from the reactant reservoir while the carrier stream contained no dye. The total volumetric flow after the mixing point was approximately equal

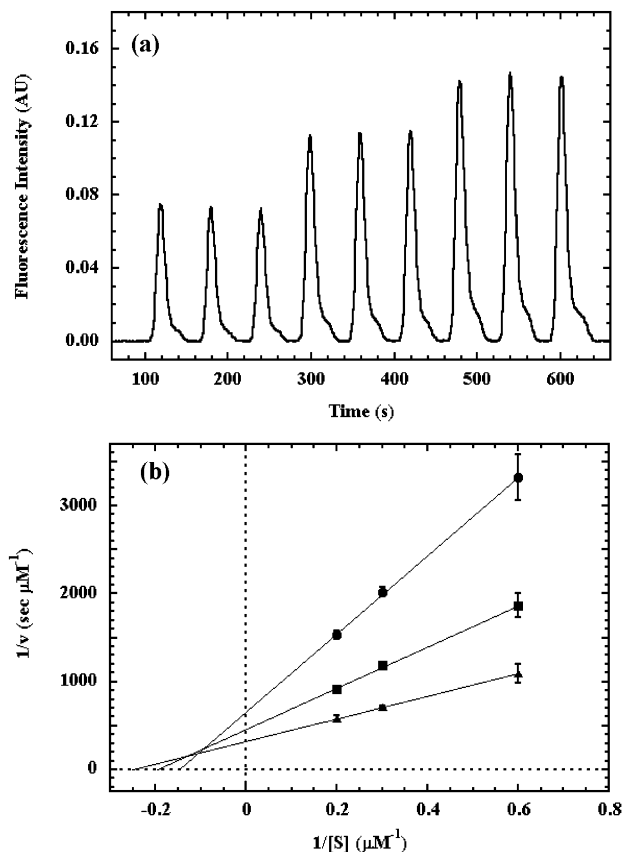


Figure 7. (a) Reaction of 3.3, 6.7, and 10.0 μM fluorescein diphosphate with 0.1 mg L^{-1} alkaline phosphatase. All solutions were made in 10 mM borate buffer (pH 9.1). Fluorescence was measured at 78.25 mm after the mixing point with a pump rate of 5.0 Hz. (b) Lineweaver-Burk double-reciprocal plot of fluorescein diphosphate reactions with (●) 0.1, (■) 0.2, and (▲) 0.3 mg L^{-1} alkaline phosphatase. Lines represent the best-fit regression of the data points. Error bars denote three times the standard deviation of the transient peak areas.

to the sum of flows from the two individual pumps, or $\sim 40 \text{ nL min}^{-1}$. Mixing was considered complete when the fluorescence intensity was homogeneous across the entire width of the microfluidic channel. Fluorescein-labeled bovine serum albumin (MW = 65 000) was found to mix after 20 s, in good agreement with a reported diffusion coefficient of $6.3 \times 10^{-7} \text{ cm}^2 \text{ s}^{-1}$,¹⁷ and diffusion distance of 50 μm (half of the 100- μm -wide channel). Diffusion was found to provide sufficient mixing for all experiments examined in this study, but for extremely large molecule or particles, more complicated channel geometries could easily be incorporated to enhance mixing.

Enzymatic Assay. The hydrolysis of fluorescein diphosphate (FDP) by alkaline phosphatase (AP) demonstrates the utility of this microfluidic FIA device for rapid chemical assays. Figure 7a shows the on-column reaction of three concentrations of FDP with 0.1 mg L^{-1} AP in 10 mM borate buffer. This reaction was monitored 78.25 cm from the point of initial mixing, corresponding to reaction time of 110 s. Peak area reproducibility was found to better than 3% relative standard deviation. In the 600 s required to collect the data seen in Figure 7a, 200 nL of enzyme was consumed corresponding to 140 amol of AP.

- (18) Chou, H. P.; Unger, M. A.; Quake, S. R. *Biomed. Microdevices* **2001**, *3*, 323–330.
- (19) Liu, R. H.; Stremmer, M. A.; Sharp, K. V.; Olsen, M. G.; Santiago, J. G.; Adrian, R. J.; Aref, H.; Beebe, D. J. *J. Microelectromech. Syst.* **2000**, *9*, 190–197.
- (20) Stroock, A. D.; Dertinger, S. K. W.; Ajdari, A.; Meziti, I.; Stone, H. A.; Whitesides, G. M. *Science* **2002**, *295*, 647–651.
- (21) Johnson, T. J.; Ross, D.; Locascio, L. E. *Anal. Chem.* **2002**, *74*, 45–51.

Table 1. Fluorescein Diphosphate-Alkaline Phosphatase Reaction Kinetics

reaction time (s)	V_{\max} (nM s ⁻¹)	K_m (μM)	k_{cat} (s ⁻¹)
Enzyme Concentration: 0.1 mg L ⁻¹			
55.0	1.4 ± 0.9	5.5 ± 4.0	39 ± 30
109.5	1.5 ± 0.5	6.8 ± 2.0	43 ± 10
Enzyme Concentration: 0.2 mg L ⁻¹			
55.0	2.4 ± 0.5	6.6 ± 1.0	34 ± 7
109.5	2.2 ± 0.5	5.1 ± 1.0	30 ± 7
Enzyme Concentration: 0.3 mg L ⁻¹			
55.0	3.1 ± 1.0	4.9 ± 2.0	29 ± 10
109.5	3.1 ± 0.7	4.0 ± 1.0	29 ± 7

A Lineweaver–Burk plot (Figure 7b) was used to calculate kinetic values for the reaction of FDP with AP.²² In this graphical representation, the x-intercept corresponds to the negative reciprocal of the Michaelis–Menten constant (K_m), while the slope is equal to K_m divided by the maximum enzyme velocity (V_{\max}). The enzymatic rate constant (k_{cat}) is determined by dividing V_{\max} by the enzyme concentration. Table 1 summarizes the kinetic values calculated for the hydrolysis of FDP by three concentrations of AP generated with the microfluidic FIA system. The average figures of 2.3 nM s⁻¹, 5.5 μM, and 34 s⁻¹ were measured for V_{\max} , K_m , and k_{cat} , respectively.

The successful kinetic characterization of alkaline phosphatase reactions has been limited by several enzyme-related factors.²³ Bovine intestinal mucosa alkaline phosphatase has been shown to exist as several isoenzymes differing in their degree of

glycosylation.²⁴ The level of glycosylation has been shown to affect enzyme V_{\max} and K_m values.²⁵ Additionally, enzymatic efficiency of AP is strongly dependent upon pH, with maximum reactivity achieved at pH 10. Buffer composition and the presence of supplemental electrolytes have also been shown to dramatically affect the activity of AP. Although no consensus exists for the efficiency of alkaline phosphatase reactions, k_{cat} has been typically calculated to be on the order of 100 s⁻¹.^{26,27} The fact that the k_{cat} value determined in this study was one-third of the generally accepted figure can be rationalized by the lack of enzyme purification, nonoptimal pH (9.1 in this study), and use of borate buffer, which has been shown to depress enzyme activity.²³ Additionally, the limited range of concentrations used in Figure 7b for the determination of these values will limit the accuracy and precision of the measurements.

Importantly, the similarity of kinetic values determined for different reaction times (measured at different points along the mixing column, see Table 1) shows that the relatively low diffusion coefficient of 2×10^{-7} cm s⁻¹²⁸ for alkaline phosphatase (MW ~ 140 000) did not impair this assay. As expected, the much smaller fluorescein diphosphate molecules were able to diffuse quickly through the reaction region to provide a continuous source of substrate. Many chemical assays rely on small reagents. Consequently, the relatively low diffusion rates of proteins and DNA fragments should not limit the possible applications of this FIA device.

ACKNOWLEDGMENT

A.M.L. thanks the National Institute of Health (NIH) for a postdoctoral fellowship. The microfluidic chips used in this project were manufactured by Fluidigm Corp. through their foundry services program, and we have benefited from numerous discussions with Mike Lee and Ian Manger. This study is supported in part by Beckman-Coulter, Inc.

Received for review September 5, 2002. Accepted December 11, 2002.

AC026112L

- (22) Copeland, R. A. *Enzymes*, 2nd ed.; Wiley-VCH: New York, 2000.
 (23) McComb, R. B.; Bowers, G. N.; Posen, S. *Alkaline Phosphatase*; Plenum Press: New York, 1979.
 (24) Enström, L. *Biochim. Biophys. Acta* **1961**, 52, 36–48.
 (25) Varki, A. *Glycobiology* **1993**, 3, 97–130.
 (26) Horton, H. R.; Moran, L. A.; Ochs, R. S.; Rawn, J. D.; Scrimgeour, K. G. *Principles of Biochemistry*; Prentice Hall, Inc.: Upper Saddle River, NJ, 1996.
 (27) Craig, D. B.; Arriaga, E. A.; Wong, J. C. Y.; Lu, H.; Dovichi, N. J. *J. Am. Chem. Soc.* **1996**, 118, 5245–5253.
 (28) Mathies, J. C.; Goodman, E. D. *J. Am. Chem. Soc.* **1953**, 75, 6061–6062.